

# Scalable sub-cycle pulse generation by soliton self-compression in hollow capillary fibers with a decreasing pressure gradient

Marina Fernández Galán\*, Enrique Conejero Jarque, and Julio San Roman

*Grupo de Investigación en Aplicaciones del Láser y Fotónica, Departamento de Física Aplicada, Universidad de Salamanca, E-37008, Salamanca, Spain*

\*e-mail: marinafergal@usal.es

Shortened version of the title: Scaling subcycle pulse generation in hollow fibers with decreasing pressure

**Abstract:** Advances in the generation of the shortest optical laser pulses down to the sub-cycle regime promise to break new ground in ultrafast science. In this work, we theoretically demonstrate the potential scaling capabilities of soliton self-compression in hollow capillary fibers with a decreasing pressure gradient to generate near-infrared sub-cycle pulses in very different dispersion and nonlinearity landscapes. Independently of input pulse, gas and fiber choices, we present a simple and general route to find the optimal self-compression parameters which result in high-quality pulses. The use of a decreasing pressure gradient naturally favors the self-compression process, resulting in shorter and cleaner sub-cycle pulses, and an improvement in the robustness of the setup when compared to the traditional constant pressure approach.

**Keywords:** ultrafast nonlinear optics, hollow capillary fibers, soliton-self compression, sub-cycle pulses.

In a continuous effort to access the briefest and most fundamental phenomena in nature, intense ultrashort laser pulses have become indispensable tools for ultrafast science, breaking new ground in time-resolved spectroscopy and strong-field physics [1,2]. At present, few-cycle femtosecond pulses in the optical spectral region are routinely generated by nonlinear post-compression in gas-filled hollow capillary fibers (HCFs) [3], which stand out among other compression schemes for their simplicity, high-damage threshold and the possibility of tuning their nonlinearity and dispersion by modifying the filling gas or its pressure. However, although HCF post-compression experiments have been greatly optimized [4], they are currently reaching their limit in terms of the shortest achievable pulse duration due to the complexity of dealing with uncompensated high-order dispersion in octave-spanning spectra. Overcoming this problem, parametric light-field synthesizers have succeeded in generating the shortest optical laser pulses well down into the sub-cycle regime, offering new opportunities for advancing real-time observation and precision control of electron dynamics at the atomic scale [5,6]. As a promising alternative to these extremely complex systems, high-energy soliton dynamics in HCFs is attracting a great interest as a direct route to extreme pulse self-compression down to the sub-cycle regime [7,8]. As opposed to more conventional post-compression techniques, soliton self-compression relies on the simultaneous nonlinear spectral broadening and phase compensation arising from the interplay between

33 the negative group-velocity dispersion (GVD) of the waveguide and self-phase modulation (SPM). Still, for a  
34 practical implementation, the complexity of this nonlinear interaction calls for theoretical investigations on  
35 scaling rules and design guidelines to identify the optimal experimental parameters which result in high-quality  
36 self-compression [9]. So far, extreme soliton self-compression in HCFs in the near-infrared (NIR) has only  
37 been demonstrated for pre-compressed ( $\sim 10$  fs) pump pulses [7,10], or otherwise in configurations which  
38 ensure a strong anomalous response, i.e., working with longer wavelengths [8,11], high-order modes [12], or  
39 small-core photonic crystal fibers [9,13]. However, the unexpected applicability of sub-cycle self-compression  
40 to standard experimental setups driven by NIR multi-cycle pulses propagating in the fundamental mode of  
41 large-core HCFs has been recently demonstrated in negatively pumped fibers, i.e., HCFs filled with a  
42 decreasing pressure gradient [14]. **Pressure gradients are routinely implemented by sealing the fiber into a gas  
43 cell at each end, which can be independently evacuated and filled with gas, yielding a longitudinal pressure  
44 distribution with a square root-type profile when the gas flows from highest to lowest pressure [10].**

45 In this Communication we further investigate the scalability of soliton self-compression down to the sub-cycle  
46 regime in HCFs filled with a decreasing pressure gradient. Varying the filling gas and choosing between atomic  
47 (Ne) and molecular ( $N_2$ ) species, we study the compression process in two completely different dispersion and  
48 nonlinearity landscapes, which are of critical importance in soliton dynamics. Our results demonstrate that  
49 nearly identical self-compression performance can be achieved in very distinct HCF scenarios, and provide a  
50 surprisingly simple universal route to find the optimal parameters for generating high-quality NIR sub-cycle  
51 pulses.

52 Our work is based on one-dimensional numerical simulations of nonlinear pulse propagation [15,16], including  
53 the complete linear response of the gas-filled HCF [17], SPM, stimulated Raman scattering modeled in a  
54 damped harmonic oscillator approximation [18], and self-steepening. This theoretical model accurately  
55 describes ultrashort pulse propagation down to the single-cycle limit in a regime of moderate intensities [19].  
56 In order to identify a route towards high-quality self-compression, we have followed the procedure detailed in  
57 [14]. In brief, we have systematically simulated the propagation of a transform-limited 30 fs gaussian pump  
58 pulse at 800 nm in the fundamental mode of a 3 m long, 100  $\mu\text{m}$  core radius HCF, filled with either Ne or  $N_2$ ,  
59 and with both constant gas pressure and a longitudinal decreasing pressure gradient ending in vacuum. The  
60 latter two situations are fairly compared by matching the integrated nonlinear phase shift acquired by the pulse  
61 peak during its propagation, which is often referred to as B-integral. Neglecting the fiber losses, a system with  
62 a decreasing pressure gradient from  $p_0$  to vacuum can then be compared to that with a constant pressure  $p_{\text{eq}}$   
63 simply if  $p_0 = 3p_{\text{eq}}/2$  [10,12]. The main difference lies in that non-uniform pressure allows for a dynamic  
64 tuning of the dispersion and nonlinearity experienced by the pulse during its self-compression, as the  
65 propagation constant and the nonlinear parameter scale linearly with the gas density and, thus, with pressure.  
66 For the parameters considered in our study, Fig. 1 shows the GVD and instantaneous nonlinear coefficient  
67 (related only to instantaneous Kerr effect or SPM [15]) of a HCF filled with Ne or  $N_2$  at different pressures.  
68 As we can see, a Ne-filled HCF has a weaker instantaneous nonlinearity and displays anomalous dispersion

69 (GVD < 0) over a larger pressure range than an identical fiber filled with N<sub>2</sub>. An inner fiber radius of 100 μm  
 70 was chosen because it offers a good balance between acceptable losses at 800 nm and a sufficiently strong  
 71 anomalous response in N<sub>2</sub>. Furthermore, a pulse propagating in N<sub>2</sub> might experience a delayed molecular  
 72 contribution to the optical Kerr effect which vanishes in noble gases like Ne. Therefore, owing to their very  
 73 distinct linear and nonlinear nature, the optimal self-compression in either Ne or N<sub>2</sub> is expected to occur for  
 74 different input pulse and fiber parameters.

75 Following [14], we have simulated the soliton self-compression of the aforementioned 30 fs pulse while  
 76 varying its initial energy and the equivalent gas pressure in the HCF. For each energy-pressure pair in the  
 77 resulting bi-dimensional parameter space, we have plotted the intensity full width at half-maximum (FWHM)  
 78 duration and the ratio of output to input peak power of the self-compressed pulses, as shown in Fig. 2. In these  
 79 plots, the optimal region for high-quality self-compression can be readily identified as the intersection between  
 80 the areas of shortest output pulse duration and largest peak power enhancement. Surprisingly, the results for  
 81 Ne and N<sub>2</sub> show an identical behavior, which also follows that previously reported for Ar [14], except for the  
 82 fact that they are displaced to different input energy and gas pressure ranges as mentioned earlier. In both cases,  
 83 it is clear that, in the whole parameter ranges considered here, the self-compression process is substantially  
 84 enhanced when the fiber is negatively pumped rather than statically filled, resulting in the generation of self-  
 85 compressed pulses with extremely short durations well down into the sub-cycle regime (~1 fs) and high peak  
 86 powers, which in turn implies a clean temporal profile. The most outstanding feature is that there is not just a  
 87 single pair of input energy and gas pressure values that allow for a high-quality compression, but there is a  
 88 whole parameter region which yields similar results. This optimal region is found to always appear towards  
 89 the same corner of the contour line in the energy-pressure map where the fixed fiber length ( $L$ ) matches an  
 90 average compression length ( $L_{av}$ ), that we defined as:

$$L_{av} = \frac{L_{sc} + L_{fiss}}{2} \quad (1)$$

91 where  $L_{sc}$  and  $L_{fiss}$  represent, respectively, the characteristic self-compression and soliton fission lengths,  
 92 which are given by [20]:

$$L_{fiss} = \frac{L_D}{N} ; L_{sc} = \frac{L_{fiss}}{\sqrt{2}} \quad (2)$$

93  $N = (L_D/L_{NL})^{1/2}$  being the soliton order, and  $L_D = T_p^2/(4 \ln 2 |\beta_2|)$  the dispersion and  $L_{NL} = 1/(\gamma_i P_0) =$   
 94  $\sqrt{\pi/(4 \ln 2)} T_p/(\gamma_i E_0)$  the nonlinear lengths, which describe the characteristic length scales of GVD and  
 95 SPM, respectively. Here  $T_p$  represents the intensity FWHM duration of the gaussian pump pulse,  $P_0$  is its input  
 96 peak power and  $E_0$  its initial energy,  $\beta_2$  is the GVD coefficient of the HCF, and  $\gamma_i$  is the instantaneous nonlinear  
 97 parameter as defined elsewhere [15]. The constraint  $L = L_{av}$  ensures that  $L_{sc} < L < L_{fiss}$  and, therefore,  
 98 guarantees that the self-compressing pulse reaches its maximum compression without entering in the soliton  
 99 fission regime. In addition, the soliton order should be kept  $N < 15$  to achieve a high-quality compression

100 [13], inevitably setting an upper limit to the achievable pulse energy. Independently of input pulse, gas and  
101 fiber parameters, the condition  $L = L_{av}$  always describes a contour line in the energy-pressure plane which,  
102 when falling inside the space with  $N < 15$ , can be used to identify the optimal region for high-quality self-  
103 compression in a universal way. A detailed inspection of the conditions  $L = L_{av}$  and  $N < 15$  suggests that  
104 upscaling our results towards millijoule pump pulses should become possible, even in practical short fibers  
105 ( $\sim 1$  m), by pushing the central wavelength into the mid-infrared spectral region.

106 As an example of the high-quality sub-cycle waveforms that can be generated from the negatively pumped  
107 fiber, in Fig. 3 we have plotted the self-compressed pulses obtained for two different pairs of input pulse energy  
108 and equivalent gas pressure which lie towards the same area of the optimal self-compression regions in Fig. 2,  
109 corresponding to Ne and N<sub>2</sub>, respectively. When compared to the output pulses in the equivalent constant  
110 pressure situations, it is clear that those generated with a decreasing gradient are much better, displaying shorter  
111 durations, higher peak powers, a cleaner temporal profile with a higher contrast, and a broader spectrum  
112 spanning from the NIR to the mid-ultraviolet. The self-compressed pulses from the negatively pumped HCF  
113 reach sub-cycle FWHM durations of 1.1 and 1.2 fs, and output peak powers of 8.8 and 10.7 GW in Ne and N<sub>2</sub>,  
114 respectively. However, in the equivalent constant pressure situations, the output pulses were only 2.2 and 2.3  
115 fs in duration, and 4.6 and 5.4 GW in peak power. The improvement with the decreasing pressure gradient has  
116 been attributed to an effective suppression of higher-order dispersion and self-steepening in the last stages of  
117 the pulse compression, together with a continuous blue-shift of the zero-dispersion frequency at the same as  
118 the pulse spectrum broadens by SPM [12,14]. When propagating in the anomalous dispersion regime, it is  
119 straightforward to understand from the trends shown in Fig. 1 that a decreasing pressure gradient is the most  
120 natural way to emphasize and favor the characteristic dynamics of the self-compression process [11]. In short,  
121 at the fiber entrance the higher pressure enhances the accumulation of nonlinear phase shift and the spectral  
122 broadening of the input pulse by SPM. In later stages, the larger spectral extent combined with an increase in  
123 the magnitude of the anomalous GVD and a reduction of third-order dispersion due to the drop in pressure,  
124 assist the phase compensation for pulse self-compression and delay the fission process beyond the maximum  
125 compression point that can be reached with constant pressure. Altogether, the decreasing pressure gradient  
126 enables unprecedented compression ratios ( $\gtrsim 25$ ) which had remained out of reach due to detrimental high-order  
127 effects [13]. Furthermore, the great similarities between the pulses in Fig. 3, generated with different gases,  
128 energies and pressures, demonstrates the promising scaling capabilities of HCF self-compression down to the  
129 sub-cycle regime in different configurations. Another interesting point is that the optimal self-compressed  
130 pulse is accompanied by the onset of resonant dispersive wave (RDW) emission, when the strongly nonlinear  
131 self-compressing soliton transfers its excess energy to a linear wave propagating in the normal dispersion  
132 regime [7,8,10,16]. This is manifested by the isolated peak around 200 nm in the output spectra of the lower  
133 panels in Fig. 3. At this point, RDW emission has just started and the energy transfer to the ultraviolet is still  
134 low, resulting in conversion efficiencies quite below saturation. This fact could be used to experimentally  
135 predict the best sub-cycle pulse parameters based on RDW spectral content at the fiber output.

136 In summary, we have demonstrated that broadly similar high-quality NIR sub-cycle pulses can be generated  
137 by extreme soliton self-compression in negatively pumped HCFs in different configurations. Independently of  
138 input pulse, gas and fiber choices, the optimal self-compression parameters can always be found by matching  
139 the fiber length to and average compression length, providing a simple design guideline for experiments.  
140 Furthermore, the decreasing pressure gradient can help to improve the robustness of HCF self-compression  
141 and the quality of the generated sub-cycle pulses when compared to the equivalent constant pressure situations,  
142 also preventing the onset of undesirable high-order effects. We believe that these findings will pave the way  
143 towards a new generation of ultrafast experiments which might benefit from the availability of tailored sub-cycle  
144 waveforms, especially those which are carried out in vacuum chambers, like the synthesis of high-frequency  
145 isolated attosecond pulses through high-order harmonic generation.

146 *Acknowledgments:* authors acknowledge financial support from Ministerio de Ciencia e Innovación under  
147 grant PID2019-106910GB-I00 funded by MCIN/AEI/10.13039/501100011033. M.F.G. acknowledges support  
148 from Ministerio de Universidades under grant FPU21/02916.

149

## 150 **References**

- 151 [1] M. Maiuri, M. Garavelli, G. Cerullo, Ultrafast spectroscopy: state of the art and open challenges, *J. Am.*  
152 *Chem. Soc.* **142**, 3 (2020).
- 153 [2] P.B. Corkum, F. Krausz, Attosecond science, *Nat. Phys.* **3**, 381 (2007).
- 154 [3] M. Nisoli, S. De Silvestri, O. Svelto, Generation of high energy 10 fs pulses by a new pulse compression  
155 technique, *Appl. Phys. Lett.* **68**, 2793 (1996).
- 156 [4] F. Silva *et al.*, Strategies for achieving intense single-cycle pulses with in-line post-compression setups,  
157 *Opt. Lett.* **43**, 337 (2018).
- 158 [5] M.T. Hassan *et al.*, Optical attosecond pulses and tracking the nonlinear response of bound electrons,  
159 *Nature* **530**, 66 (2016).
- 160 [6] G.M. Rossi *et al.*, Sub-cycle millijoule-level parametric waveform synthesizer for attosecond science, *Nat.*  
161 *Photon.* **14**, 629 (2020).
- 162 [7] J.C. Travers *et al.*, High-energy pulse self-compression and ultraviolet generation through soliton dynamics  
163 in hollow capillary fibers, *Nat. Photon.* **13**, 547 (2019).
- 164 [8] C. Brahms, F. Belli, J.C. Travers, Infrared attosecond field transients and UV to IR few-femtosecond pulses  
165 generated by high-energy soliton self-compression, *Phys. Rev. Res.* **2**, 043037 (2020).
- 166 [9] D. Schade *et al.*, Scaling rules for high quality soliton self-compression in hollow-core fibers, *Opt. Express*  
167 **29**, 19147 (2021).

- 168 [10] C. Brahms, F. Belli, J.C. Travers, Resonant dispersive wave emission in hollow capillary fibers filled with  
169 pressure gradients, *Opt. Lett.* **45**, 4456 (2020).
- 170 [11] A.A. Voronin, A.M. Zheltikov, Subcycle solitonic breathers, *Phys. Rev. A* **90**, 043807 (2014).
- 171 [12] Y. Wan, W. Chang, Effect of decreasing pressure on soliton self-compression in higher-order modes of a  
172 gas-filled capillary, *Opt. Express* **29**, 7070 (2021).
- 173 [13] A.A. Voronin, A.M. Zheltikov, Soliton-number analysis of soliton-effect pulse compression to single-  
174 cycle pulse widths, *Phys. Rev. A* **78**, 063834 (2008).
- 175 [14] M.F. Galán, E.C. Jarque, J. San Roman, Optimization of pulse self-compression in hollow capillary fibers  
176 using decreasing pressure gradients, *Opt. Express* **30**, 6755 (2022).
- 177 [15] G.P. Agrawal, *Nonlinear Fiber Optics*, 5th edn. (Academic Press, 2013).
- 178 [16] A. Crego, J. San Roman, E.C. Jarque, Tools for numerical modelling of nonlinear propagation in hollow  
179 capillary fibres and their application, *J. Opt.* **25**, 024005 (2023).
- 180 [17] E.A.J. Macatili, R.A. Schmelzter, Hollow metallic and dielectric waveguides for long distance optical  
181 transmission and lasers, *Bell Syst. Tech. J.* **43**, 1783 (1964).
- 182 [18] P.A. Carpeggiani *et al.*, Extreme Raman red shift: ultrafast multimode nonlinear space-time dynamics,  
183 pulse compression, and broadly tunable frequency conversion, *Optica* **7**, 1349 (2020).
- 184 [19] T. Brabec, F. Krausz, Nonlinear optical pulse propagation in the single-cycle regime, *Phys. Rev. Lett.* **78**,  
185 3282 (1997).
- 186 [20] C.M. Chen, P.L. Kelley, Nonlinear pulse compression in optical fibers: scaling laws and numerical  
187 analysis, *J. Opt. Soc. Am. B* **19**, 1961 (2002).

## Figure captions:

**Figure 1.** GVD (top) and instantaneous nonlinear coefficient (bottom) at 800 nm of the fundamental mode of a 100  $\mu\text{m}$  core radius HCF filled with Ne or  $\text{N}_2$  as a function of gas pressure. Labels indicate the zero-dispersion pressure ( $p_{ZD}$ ) in each case.

**Figure 2.** FWHM duration (top row) and ratio of output to input peak power (bottom row) of the self-compressed pulses as a function of the input energy and the equivalent constant pressure (see text) in both a statically filled or a negatively pumped 3 m long, 100  $\mu\text{m}$  core radius HCF filled with Ne (left) or  $\text{N}_2$  (right). The solid black lines represent the contour lines where  $L = L_{av}$ , which run along the optimal region for self-compression in a decreasing pressure gradient. Note the one order of magnitude change in the pressure range from Ne to  $\text{N}_2$  owing to their different dispersion and nonlinearity.

**Figure 3.** Temporal intensity profile (top row) and spectrum (bottom row) of the self-compressed sub-cycle pulses obtained after propagation through a HCF filled with Ne (left) or  $\text{N}_2$  (right), at both constant or decreasing pressure, for two different pairs of input pulse energy and equivalent gas pressure which lie towards the same area of the optimal self-compression regions in [Fig.2](#).

# Figures:

FIGURE 1:

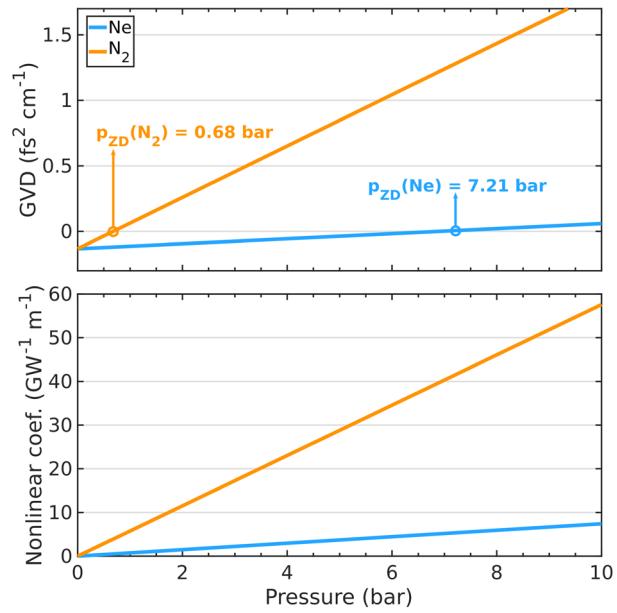


FIGURE 2:

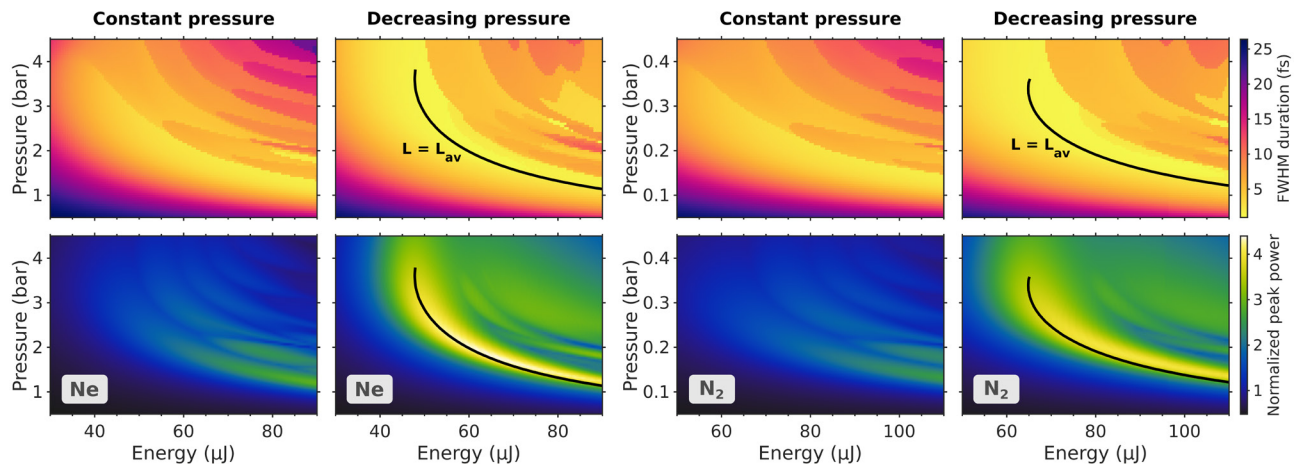




FIGURE 3:

